Bilateral Comparison of 1.018 V and 10 V Standards
between the INTI (Argentina) and the BIPM,
August to October 2009
(part of the ongoing BIPM key comparison BIPM.EM-K11.a and b)

by A.Tonina*, R.Iuzzolino*, M.Bierzychudek* and M.Real*
S. Solve+ R. Chayramy+ and M. Stock+

* Instituto Nacional de Tecnologia Industrial (INTI), Buenos Aires, Argentina

+ Bureau International des Poids et Mesures, F-92312 Sèvres Cedex

Introduction

As a part of the ongoing BIPM key comparison BIPM.EM-K11.a and b, a comparison of the 1.018 V and 10 V voltage reference standards of the BIPM and the Instituto Nacional de Tecnologia Industrial (INTI), Buenos Aires, Argentina, was carried out from August to October 2009. Two BIPM Zener diode-based travelling standards (Fluke 732B), BIPM_7 (SN: 6615014) and BIPM_8 (SN: 6625014), were transported by freight to INTI. The INTI measurements were carried out by direct comparison to the JVS at 1.018 V and through a voltage divider at 10 V.

At the BIPM, the traveling standards were calibrated at both voltages before and after the measurements at INTI, with the Josephson Voltage Standard. Results of all measurements were corrected for the dependence of the output voltages on internal temperature and ambient pressure.

Results at 1.018 V

Figure 1 shows the measured values obtained for the two standards by the two laboratories at 1.018 V. A linear least squares fit is applied to the results of the BIPM to obtain the results for both standards and their uncertainties at the mean date of INTI measurements as a common reference date.

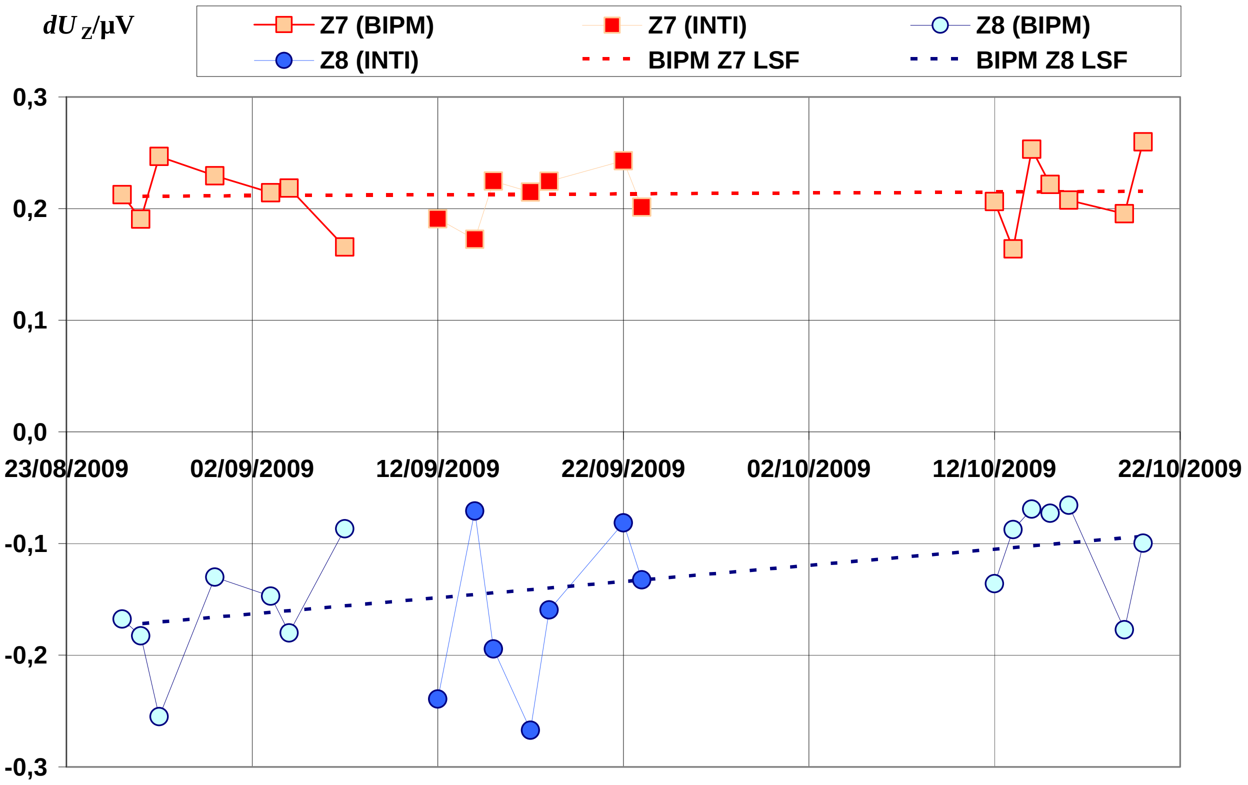

Figure 1. Voltage of BIPM_7 (in red) and BIPM_8 (in blue) at 1.018 V measured at both institutes, referred to an arbitrary origin, as a function of time, with a linear least-squares fit to the measurements of the BIPM.

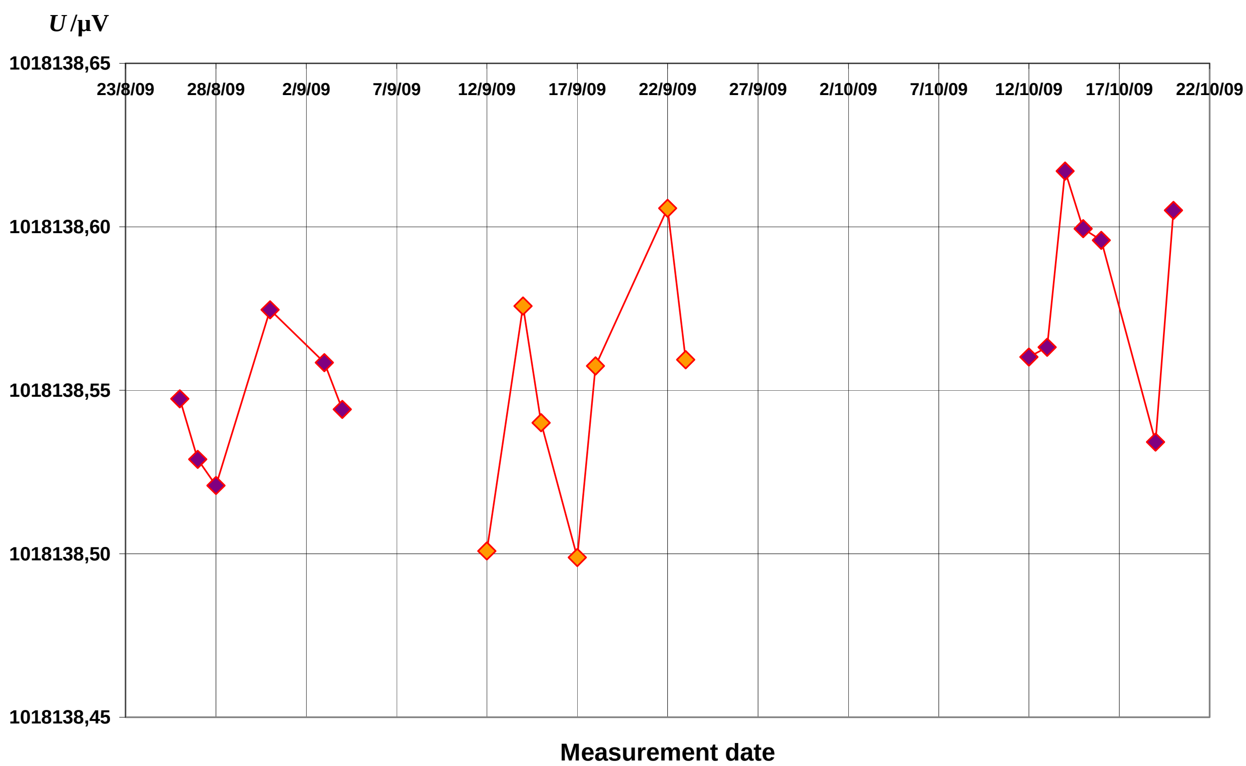

Figure 2. Voltage evolution of the simple mean of the two standards at 1.018 V.

Table 1 lists the results of the comparison and the uncertainty contributions for the comparison INTI/BIPM at 1.018 V. Experience has shown that flicker or 1/*f* noise ultimately limits the stability characteristics of Zener diode standards and it is not appropriate to use the standard deviation divided by the square root of the number of observations to characterize the dispersion of measured values. For the present standards, the relative value of the voltage noise floor due to flicker noise is about 1 part in 10^8.

In estimating the uncertainty related to the stability of the standards during transportation, we have calculated the "*a priori*" uncertainty of the mean of the results obtained for the two standards (also called statistical internal consistency). It consists of the quadratic combination of the uncorrelated uncertainties of each result. We compared this component to the "*a posteriori*" uncertainty (also called statistical external consistency) which consists of the experimental standard deviation of the mean of the results from the two traveling standards[*]. If the "*a posteriori*" uncertainty is significantly larger than the "*a priori*" uncertainty, we assume that a standard has changed in an unusual way and we use the larger of these two estimates in calculating the final uncertainty.

In Table 1, the following elements are listed:

(1) the value attributed by INTI to each Zener U_{INTI} , computed as the simple mean of all data from INTI;

(2) the Type A uncertainty due to the instability of the Zener, computed as the standard uncertainty of the value predicted by the linear drift model for the mean date, or as an estimate of the 1/*f* noise voltage level, whichever is greater;

(3) the uncertainty component arising from the maintenance of the volt at INTI: this uncertainty is completely correlated between the different Zeners used for a comparison;

(4-6) the corresponding quantities for the BIPM referenced to the mean date of the INTI measurements;

(7) the uncertainty due to the combined effects of the uncertainties of the pressure and temperature coefficients and to the differences of the mean pressures and

[*] With only two traveling standards, the uncertainty of the standard deviation of the mean is comparable to the value of the standard deviation of the mean itself.

temperatures in the participating laboratories is calculated using the following assumption:

Traditionally, an average of the uncertainties of the temperature coefficients of both Zener standards is calculated. The uncertainty on the temperature correction is then considered for the difference between the mean values of the temperature measured at both institutes.

$u_T = U \times u(c_T) \times \Delta R$ where U= 1.018 V, $u(c_T) = 1.36\times10^{-7}$ /kΩ,. ΔR= 0.02 kΩ for Z7 and ΔR = 0.02 kΩ for Z8.

The same procedure is applied for the uncertainty on the pressure correction for the difference between the mean values of the pressure measured at both institutes:

$u_P = U \times u(c_P) \times \Delta P$ where U= 1.018 V $u(c_P) = 0.04\times10^{-9}$ /hPa, ΔP= 5.4 hPa for Z7 and ΔP= 5.5 hPa for Z8.

The last evaluation of the correction coefficient was carried out in 1997 and it is obvious to suspect that the coefficient has changed since then.

We have thus decided to apply an expansion coefficient of 3 to the component to take into account the possible change of the coefficient of the temperature correction.

(8) the difference (U_{INTI} — U_{BIPM}) for each Zener, and (9) the uncorrelated part of the uncertainty;

(10) the result of the comparison is the simple mean of the differences of the calibration results for the different standards;

(11 and 12) the uncertainty related to the transfer, estimated by the following two methods:

(11) the *a priori* uncertainty, determined as described on page 3;

(12) the *a posteriori* uncertainty, which is the standard deviation of the mean of the two results;

(13) the correlated part of the uncertainty and

(14) the total uncertainty of the comparison, which is the root sum square of the correlated part of the uncertainty and of the larger of (11) and (12).

Table 2a and 2b summarize the uncertainties related to the calibration of a Zener diode against the Josephson array voltage standard at the BIPM and at INTI respectively.

Table 3a and 3b list the uncertainties related to the maintenance of the volt and the Zener calibration at INTI.

The result of the comparison is presented as the difference between the value assigned to a 1.018 V standard by INTI, at INTI, U_{INTI}, and that assigned by the BIPM, at the BIPM, U_{BIPM}, which for the reference date is

$$U_{INTI} - U_{BIPM} = -0.010\ \mu V; \qquad u_c = 0.032\ \mu V \quad \text{on 2009/09/17},$$

where u_c is the combined standard uncertainty associated with the measured difference, including the uncertainty of the representation of the volt at the BIPM and at INTI, based on K_{J-90}, and the uncertainty related to the comparison.

The uncorrelated uncertainty is $w = [r^2 + t^2 + v^2]^{1/2}$, the expected transfer uncertainty (*a priori* uncertainty) is $x = ½ [w_7^2 + w_8^2]^{1/2}$, and the correlated uncertainty is $y = [s^2 + u^2]^{1/2}$, where:

r is the INTI Type A uncertainty (2);
s is the INTI Type B uncertainty, which is assumed to be correlated for both transfer standards (3);
t is the BIPM Type A uncertainty (5);
u is the BIPM Type B uncertainty, which is assumed to be correlated for both transfer standards (6);
v is the pressure and temperature coefficient correction uncertainty (7);
w_i is the quadratic combination of the uncorrelated uncertainties for the Zener (9);
x is the expected transfer uncertainty (from the calculation of the statistical internal consistency) (11);
y is the quadratic combination of the correlated uncertainties (13).

(U_Z — 1.018 V)

Table 1. Results of the INTI (Argentina)/BIPM bilateral comparison of 1.018 V standards using two Zener traveling standards: reference date 17 September 2009. Uncertainties are 1 σ estimates.

		BIPM_7	BIPM_8	
1	*INTI (Argentina)*(U_Z — 1.018 V)/µV	107.41	169.69	
2	Type A uncertainty/µV	0.01	0.03	*r*
3	correlated unc. /µV	0.01		*s*
4	*BIPM* (U_Z — 1.018 V)/µV	107.38	169.73	
5	Type A uncertainty/µV	0.01	0.02	*t*
6	correlated unc./µV	0.001		*u*
7	pressure and temperature correction uncertainty/µV	0.03	0.03	*v*
8	(U_{INTI} — U_{BIPM})/µV	0.03	-0.04	
9	uncorrelated uncertainty/µV	0.03	0.05	*w*
10	< U_{INTI} — U_{BIPM} >/µV	-0.01		
11	*a priori* uncertainty/µV	0.02		*x*
12	*a posteriori* uncertainty/µV	0.03		
13	correlated uncertainty/µV	0.01		*y*
14	comparison total uncertainty/µV	0.032		

Table 2a. Estimated standard uncertainties for Zener calibrations with the BIPM equipment at the level of 1.018 V without the contribution of the Zener noise. The comparison Type A uncertainty was calculated as the standard deviation of the mean of the BIPM daily measurement results and is equal to 13 nV.

JVS & detector uncertainty components	Uncertainty/nV
Residual thermal electromotive forces	included in the Type A uncertainty
electromagnetic interference	0.34
detector gain	0.11
leakage resistance	3×10^{-3}
frequency	3×10^{-3}
pressure and temperature correction	included in the Zener unc. budget
total	0.36

Note: We consider that this component can't be lower than the 1/f noise floor estimated at 10 nV.

Table 2b. Estimated JVS standard uncertainties for Zener calibrations with the INTI equipment at the level of 1.018 V.

1V and 1.018 V measurements / Influence factor y_i	Standard uncertainty $u(y_i)$	Distribution /method of evaluation (A, B)	Sensitivity coefficient c_i	Uncertainty contribution $u(R_i)$	Effective degrees of freedom ν_i
Voltage Reference Realization	$9.0\text{x}10^{-3}$ µV/V	Normal / A	1	$9.0\text{x}10^{-3}$ µV/V	19
Frequency	$9.8\text{x}10^{-5}$ µV/V	Rect / B	1	$9.8\text{x}10^{-5}$ µV/V	50
Detector-Gain correction	$2.9\text{x}10^{-4}$ µV/V	Rect / B	1	$2.9\text{x}10^{-4}$ µV/V	50
Leakage Resistance	$1.0\text{x}10^{-4}$ µV/V	Rect / B	1	$1.0\text{x}10^{-4}$ µV/V	5
Combined standard uncertainty and effective degrees of freedom:				**$1.0\text{x}10^{-2}$ µV/V**	**19**

Tables 3a and 3b. present the estimated standard uncertainties for Z7 and Z8 respectively for their calibration with the INTI equipment.

Table 3a. Zener z7 s/n 6615014 – 1.018 V

Influence factor y_i	Standard uncertainty $u(y_i)$	Distribution /method of evaluation (A, B)	Sensitivity coefficient c_i	Uncertainty contribution $u(R_i)$	Effective degrees of freedom ν_i
JVS	1.0×10^{-2} µV/V	Normal / B	1	1.0×10^{-2} µV/V	19
Ambient conditions					
Temperature	1.0×10^{-2} kΩ	Normal / B	5.0×10^{-1} (1/kΩ) µV/V	5.0×10^{-3} µV/V	13
Pressure	2.6×10^{-1} hPa	Normal / B	1.9×10^{-3} (1/hPa) µV/V	4.9×10^{-4} µV/V	13
Corrected Mean Value Type A standard deviation*					
Type A standard deviation	1.0×10^{-2} µV/V	Normal/A	1	1.0×10^{-2} µV/V	13
Combined standard uncertainty and effective degrees of freedom*:				1.5×10^{-2} µV/V	35

* These values were calculated only for checking purposes

Table 3b. Zener z8 s/n 6625014 – 1.018 V

Influence factor y_i	Standard uncertainty $u(y_i)$	Distribution /method of evaluation (A, B)	Sensitivity coefficient c_i	Uncertainty contribution $u(R_i)$	Effective degrees of freedom ν_i
JVS	1.0×10^{-2} µV/V	Normal / B	1	1.0×10^{-2} µV/V	19
Ambient conditions					
Temperature	1.0×10^{-2} kΩ	Normal / B	2.3×10^{-1} (1/kΩ) µV/V	2.3×10^{-3} µV/V	13
Pressure	2.6×10^{-1} hPa	Normal / B	2.1×10^{-3} (1/hPa) µV/V	5.4×10^{-4} µV/V	13
Corrected Mean Value Type A standard deviation*					
Type A standard deviation	3.0×10^{-2} µV/V	Normal/A	1	3.0×10^{-2} µV/V	13
Combined standard uncertainty and effective degrees of freedom*:				3.2×10^{-2} µV/V	16

* These values were calculated only for checking purposes

Results at 10 V

Figure 3 shows the measured values obtained for the two standards by the two laboratories at 10 V. A linear least squares fit is applied to the results of the BIPM to obtain the results for both standards and their uncertainties at the mean date of the INTI measurements.

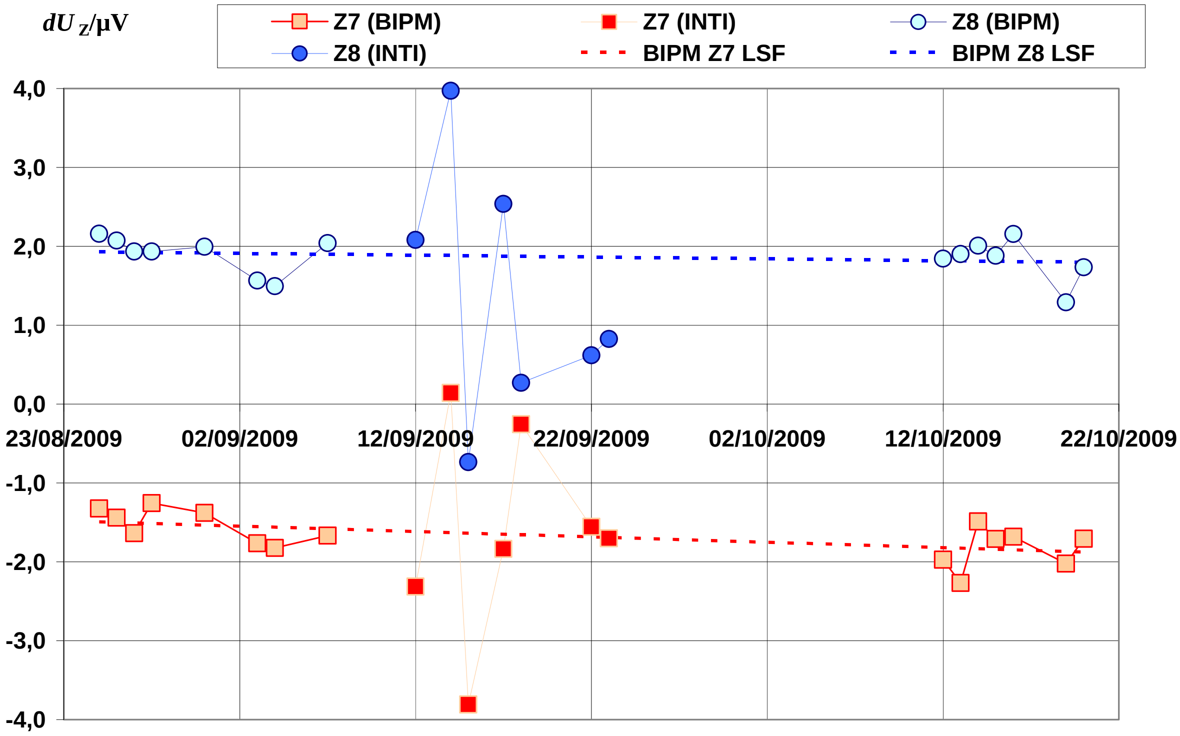

Figure 3. Voltage of BIPM_7 (in red) and BIPM_8 (in blue) at 10 V measured at both institutes, referred to an arbitrary origin, as a function of time, with a linear least-squares fit to the measurements of both laboratories.

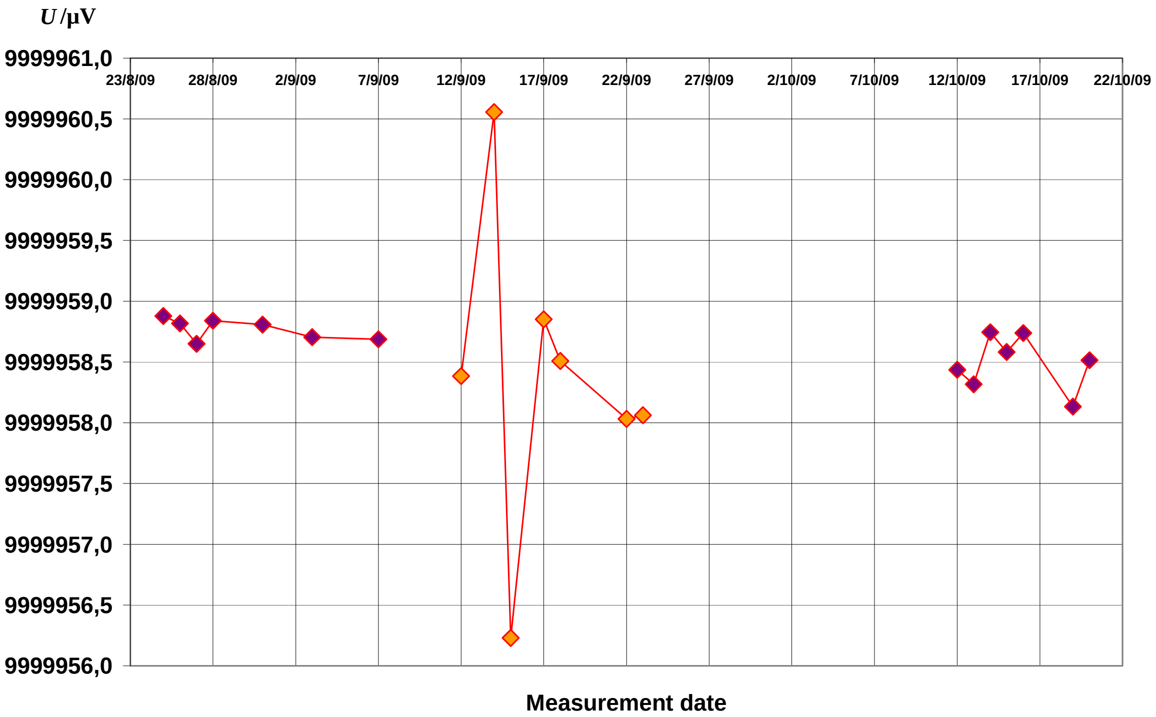

Figure 4. Voltage evolution of the simple mean of the two standards at 10 V.

Table 4 lists the results of the comparison and the uncertainty contributions for the comparison INTI/BIPM at 10 V. The relative value of the voltage noise floor due to flicker noise is about 1 part in 10^8 and represents the ultimate limit of the stability of Zener voltage standards.

In estimating the uncertainty related to the stability of the standards during transportation, we have calculated the "*a priori*" uncertainty of the mean of the results and the "*a posteriori*" uncertainty which consists of the experimental standard deviation of the mean of the results from the two traveling standards. Then we applied the same methodology as described in the measurements at 1.018 V.

In this particular case, the measurements of both standards carried out at BIPM before being shipped to INTI and after being shipped back to BIPM show a very good agreement (Cf. Fig. 3). We have selected the "*a priori*" uncertainty as the component that represents the uncertainty on the transportation. (see 11)

In Table 4, the following elements are listed:

(1) the predicted value U_{INTI} of each Zener, computed using a linear least-squares fit to all data from INTI and referenced to the mean date of INTI's measurements;
(2) the Type A uncertainty due to the instability of the Zener, computed as the standard uncertainty of the value predicted by the linear drift model, or as an estimate of the 1/*f* noise voltage level, whichever is greater;
(3) the uncertainty component arising from the maintenance of the volt at INTI: this uncertainty is completely correlated between the different Zeners used for a comparison;
(4-6) the corresponding quantities for the BIPM referenced to the mean date of INTI's measurements;
(7) the uncertainty due to the combined effects of the uncertainties of the pressure and temperature coefficients and to the difference of the mean pressures and temperatures in the participating laboratories is calculated using the following assumption:
An average of the uncertainties of the temperature coefficients of both Zener standards is calculated. The uncertainty on the temperature correction is then considered for the difference between the mean values of the temperature measured at both institutes.

$u_T = U \times u(c_T) \times \Delta R$ where U= 10 V, $u(c_T)$ = 1.01×10^{-7} /kΩ, ΔR= 0.17 kΩ for Z7 and ΔR = 0.003 kΩ for Z8.

The same procedure is applied for the uncertainty on the pressure correction for the difference between the mean values of the pressure measured at both institutes:

$u_P = U \times u(c_P) \times \Delta P$ where U= 10 V, $u(c_P)$= 0.05×10^{-9} /hPa, ΔP= 5.3 hPa for Z7 and ΔP= 5.5 hPa for Z8.

(8) the difference (U_{INTI} — U_{BIPM}) for each Zener, and (9) the uncorrelated part of the uncertainty;

(10) the result of the comparison is the simple mean of the differences of the calibration results for the different standards;

(11 and 12) the uncertainty related to the transfer, estimated by the following two methods:

(11) the *a priori* uncertainty, determined as described on page 3;

(12) the *a posteriori* uncertainty, which is the standard deviation of the mean of the two results;

(13) the correlated part of the uncertainty and

(14) the total uncertainty of the comparison, which is the root sum square of the correlated part of the uncertainty and of (11) .

Table 5 summarizes the uncertainties related to the calibration of a Zener diode against the Josephson array voltage standard at the BIPM.

Tables 6, 7a and 7b. present the estimated standard uncertainties for Z7 and Z8 respectively for their calibration with the INTI measurement setup.

The comparison result is presented as the difference between the value assigned to a 10 V standard by INTI, at INTI, U_{INTI}, and that assigned by the BIPM, at the BIPM, U_{BIPM}, which for the reference date is

$$U_{INTI} — U_{BIPM} = -0.238\ \mu V; \qquad u_c = 0.380\ \mu V \quad \text{on 2009/09/17},$$

where u_c is the combined standard uncertainty associated with the measured difference, including the uncertainty of the representation of the volt at the BIPM and at INTI, based on K_{J-90}, and the uncertainty related to the comparison.

The uncorrelated uncertainty is $w = [r^2 + t^2 + v^2]^{1/2}$, the expected transfer uncertainty (*a priori* uncertainty) is $x = ½\ [w_7^2 + w_8^2\ ]^{1/2}$, and the correlated uncertainty is $y = [s^2 + u^2]^{1/2}$, where:

r is the INTI Type A uncertainty (2);
s is the INTI Type B uncertainty, which is assumed to be correlated for both transfer standards (3);
t is the BIPM Type A uncertainty (5);
u is the BIPM Type B uncertainty, which is assumed to be correlated for both transfer standards (6);
v is the pressure and temperature coefficient correction uncertainty (7);
w_i is the quadratic combination of the uncorrelated uncertainties for the Zener (9);
x is the expected transfer uncertainty (from the calculation of the statistical internal consistency) (11);
y is the quadratic combination of the correlated uncertainties (13).

(U_Z — 10 V)

Table 4. Results of the INTI (Argentina)/BIPM bilateral comparison of 10 V standards using two Zener traveling standards: reference date 17 September 2009. Uncertainties are 1 σ estimates.

		BIPM_7	BIPM_8	
1	*INTI (Argentina)*(U_Z — 10 V)/µV	-32.62	-50.63	
2	Type A uncertainty/µV	0.5	0.5	*r*
3	correlated unc. /µV	0.12		*s*
4	*BIPM* (U_Z — 10 V)/µV	-32.65	-50.12	
5	Type A uncertainty/µV	0.1	0.1	*t*
6	correlated unc./µV	0.001		*u*
7	pressure and temperature correction uncertainty/µV	0.17	0.004	*v*
8	(U_{INTI} — U_{BIPM})/µV	0.03	-0.55	
9	uncorrelated uncertainty/µV	0.54	0.51	*w*
10	< U_{INTI} — U_{BIPM} >/µV	-0.238		
11	*a priori* uncertainty/µV	0.361		*x*
12	*a posteriori* uncertainty/µV	0.271		
13	correlated uncertainty/µV	0.12		*y*
14	comparison total uncertainty/µV	0.380		

Table 5. Estimated standard uncertainties for Zener calibrations with the BIPM equipment at the level of 10 V without the contribution of the Zener noise. The standard deviation of the mean of the BIPM daily measurement results is equal to 45

JVS & detector uncertainty components	Uncertainty/nV
Residual thermal electromotive forces	included in the Type A uncertainty
electromagnetic interference	0.86
detector gain	0.11
leakage resistance	3×10^{-2}
frequency	3×10^{-2}
pressure and temperature correction	included in the Zener unc. budget
total	0.87

Note: We consider that the Type A uncertainty can't be lower than the 1/f noise floor estimated at 100 nV.

Table 6. Estimated standard uncertainties for Zener calibrations with the INTI equipment at the level of 10 V using the voltage resistive divider

10V Influence factor y_i	Standard uncertainty $u(y_i)$	Distribution /method of evaluation (A, B)	Sensitivity coefficient c_i	Uncertainty contribution $u(R_i)$	Effective degrees of freedom ν_i
Ratio calibration (α)	$9.2\text{x}10^{-2}$ µV/V	Rect / B	0.9	$8.3\text{x}10^{-2}$ µV/V	50
Loading effect	$8.0\text{x}10^{-2}$ µV/V	Rect / B	1	$8.0\text{x}10^{-2}$ µV/V	50
Leakage	$2.0\text{x}10^{-4}$ µV/V	Rect / B	1	$2.0\text{x}10^{-4}$ µV/V	50
Combined standard uncertainty and effective degrees of freedom:				**$1.2\text{x}10^{-1}$ µV/V**	**100**

Table 7a. Zener z7 s/n 6615014 - 10 V

Influence factor y_i	Standard uncertainty $u(y_i)$	Distribution /method of evaluation (A, B)	Sensitivity coefficient c_i	Uncertainty contribution $u(R_i)$	Effective degrees of freedom ν_i
JVS	$1.0\text{x}10^{-2}$ µV/V	Normal / B	**1**	$1.0\text{x}10^{-2}$ µV/V	19
Resistive Voltage Divider	$1.2\text{x}10^{-1}$ µV/V	Rect / B	**1**	$1.2\text{x}10^{-1}$ µV/V	100
Ambient conditions					
Temperature	$1.0\text{x}10^{-2}$ kΩ	Normal / B	$1.1\text{x}10^{-2}$ (1/kΩ) µV/V	$1.1\text{x}10^{-4}$ µV/V	13
Pressure	$2.6\text{x}10^{-1}$ hPa	Normal / B	$1.9\text{x}10^{-3}$ (1/hPa) µV/V	$4.9\text{x}10^{-4}$ µV/V	13
Corrected Mean Value Type A standard deviation*					
Type A standard deviation	$5.0\text{x}10^{-2}$ µV/V	Normal/A	1	$5.0\text{x}10^{-2}$ µV/V	13
Combined standard uncertainty and effective degrees of freedom*:				**$1.2\text{x}10^{-1}$ µV/V**	**63**

* These values were calculated only for checking purposes

Table 7b. Zener z8 s/n 6625014 - 10 V

Influence factor y_i	Standard uncertainty $u(y_i)$	Distribution /method of evaluation (A, B)	Sensitivity coefficient c_i	Uncertainty contribution $u(R_i)$	Effective degrees of freedom ν_i
JVS	$1.0\text{x}10^{-2}$ µV/V	Normal / B	**1**	$1.0\text{x}10^{-2}$ µV/V	19
Resistive Voltage Divider	$1.2\text{x}10^{-1}$ µV/V	Rect / B	**1**	$1.2\text{x}10^{-1}$ µV/V	100
Ambient conditions					
Temperature	$1.0\text{x}10^{-2}$ kΩ	Normal / B	$7.8\text{x}10^{-2}$ (1/kΩ) µV/V	$7.8\text{x}10^{-4}$ µV/V	13
Pressure	$2.6\text{x}10^{-1}$ hPa	Normal / B	$2.1\text{x}10^{-3}$ (1/hPa) µV/V	$5.4\text{x}10^{-4}$ µV/V	13
Corrected Mean Value Type A standard deviation*					
Type A standard deviation	$6.0\text{x}10^{-2}$ µV/V	Normal/A	1	$5.0\text{x}10^{-2}$ µV/V	13
Combined standard uncertainty and effective degrees of freedom*:				**$1.3\text{x}10^{-1}$ µV/V**	**64**

* These values were calculated only for checking purposes

Conclusion

The final result of the comparison is presented as the difference between the value assigned to DC voltage standard by INTI, at the level of 1.018 V and 10 V, at INTI, U_{INTI}, and that assigned by the BIPM, at the BIPM, U_{BIPM}, at the reference date of the 17th of September 2009

$$U_{INTI} - U_{BIPM} = -0.01\ \mu V; \quad u_c = 0.03\ \mu V \quad \text{, at 1.018 V}$$

$$U_{INTI} - U_{BIPM} = -0.24\ \mu V; \quad u_c = 0.38\ \mu V \quad \text{, at 10 V}$$

where u_c is the combined standard uncertainty associated with the measured difference, including the uncertainty of the representation of the volt at the BIPM and at INTI, based on K_{J-90}, and the uncertainty related to the comparison.

These are very satisfactory results. The comparison results show that the voltage standards maintained by INTI and the BIPM were equivalent, within their stated expanded uncertainties, on the mean date of the comparison.

Prior to this comparison, a technical study was performed at BIPM in order to guarantee the uninterrupted power supply of the standards during their long trip to Argentina. The result of this study was the installation of an additional adequate battery that could allow the Zeners to be powered during 8 consecutive days without being plugged back to the mains. The efficiency of this system developed and tested at BIPM has been demonstrated in this comparison exercise (Cf. Appendix B).

Appendix A : Technical details on the INTI Measurement setup

Description of the measurement setup

The two zener outputs (1.018 V and 10 V) were measured with the INTI's Josephson voltage standard system (JVS). This system has been maintained at INTI since 1992. This is a 1 V JVS, which allows to measure the 1.018 V zener output in a direct way. To measure the 10 V zener output, a resistive voltage divider has been developed. This divider is based on tetrahedral junctions and sealed oil-filled commercial resistors. It uses the Hamon series-parallel method to obtain the divider ratio.

The 1.018 V zener output was measured in opposition with the JVS. An Agilent 34420 nanovoltmeter was used as null detector.

The 10 V zener output was connected to the resistive voltage divider and its output was measured in opposition with the JVS (see Figure A1). The voltage divider has an input and output resistances of 100 kΩ and 10 kΩ respectively. An Agilent 34420A nanovoltmeter was used as detector too.

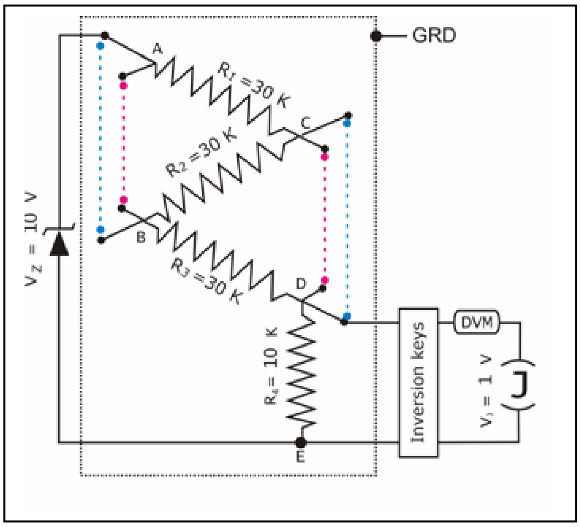

Figure A1: Diagram of connections of the resistive voltage divider to 1V-JVS and 10 V zener output

To characterize the divider, the ratio was measured before and after the JVS zener measurements with a potentiometric system, specially designed and built at INTI to calibrate high accuracy 10 kΩ standard resistors.

The zener internal thermistor was measured with a nanovoltmeter, Agilent 34420A, as four-terminal resistance measure function in low power mode. The laboratory pressure was measured with a *Paroscientific* sensor.

Measurement Procedure

The 1.018 V and 10 V outputs of each zener were measured in two to four series of twenty measurements each during seven days, starting at September, 12^{th} and finishing on September, 23^{th}. September 12^{th} was the first day of measurements, 24 hours after their arrival to the laboratory. To minimize thermal voltages and offsets a +--+ measurement sequence was made on each series, with ten measurements on each voltage reference polarity. Then a least squares algorithm was used to compute the values with minimum error.

The ambient conditions, as atmospheric pressure, room temperature, humidity and thermistors were measured before and after each JVS measurement.

Appendix B: Technical details on the experiment carried out at BIPM to monitored the longevity of the “in cal” status of Zener powered by an extra battery

The internal battery of the Zener and the external one (Valve regulated lead acid battery of 17.0 Ah) were fully charged. This last one was connected in parallel to the internal battery. A photodiode was installed in front of the LED “Low bat.” on the front panel of the Zener. The photodiode was isolated from any spurious light with a black tape which allows the photodiode to stick properly to the front panel as well.

A software was written to record the time, the voltage across the photodiode, the voltage across the powering batteries and the internal temperature of the Zener (in terms of the resistance value of a thermistor). All these data were stored in an electronic file during the experiment.

The experiment was stopped as soon as the voltage across the photodiode changed. The zener was then immediately plugged back to the mains. The conclusion is that the Zener remains properly powered over 6 days and a half (156 hours).

The results are presented in terms of three different graphs:

► Graph B1 shows the evolution of the voltage across the powering batteries (orange) in time, referred to the right scale of the graph and the voltage across the photodiode (blue) referred to the left scale as a function of time.

► Graph B2 is a zoom of the voltage across the photodiode (blue) curve as a function of time. The graph shows a slight change which is due to the activity of the Zener measurement setup.

► Graph B3 presents the evolution of the voltage across the powering batteries (orange) in time, referred to the right scale of the graph and the internal temperature of the Zener (green) referred to the left scale as a function of time.

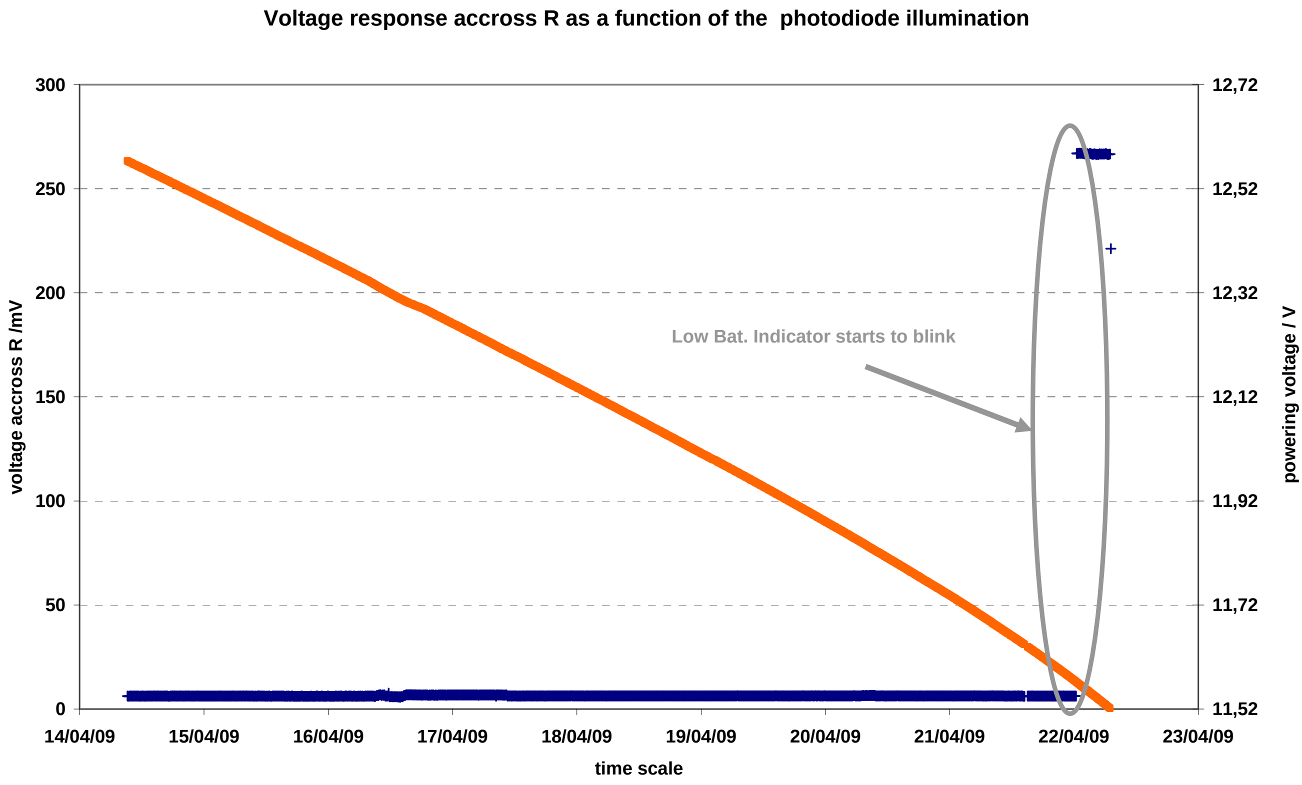

Graph B1: Evolution of the voltage across the powering batteries (orange) and voltage across the photodiode as a function of time.

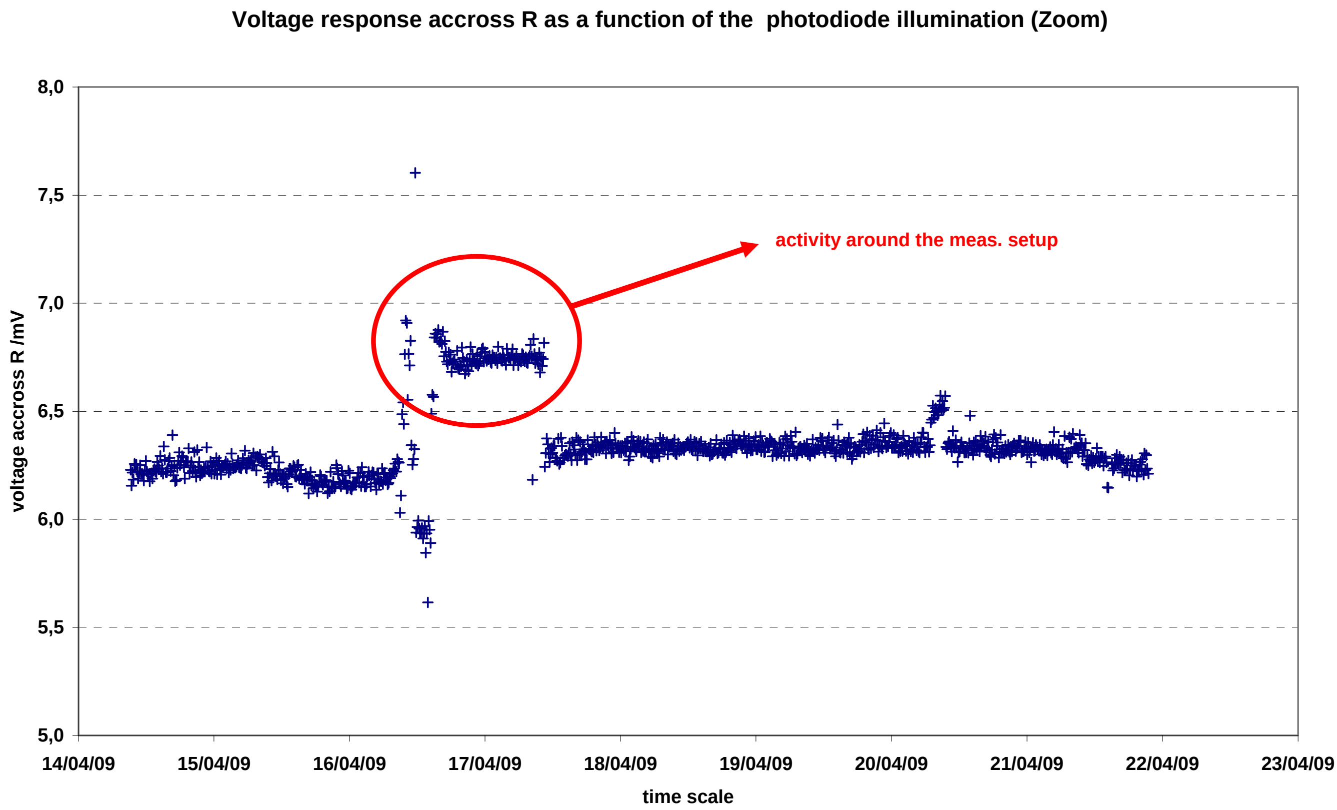

Graph B2: Zoom of the voltage across the photodiode (blue) curve as a function of time.

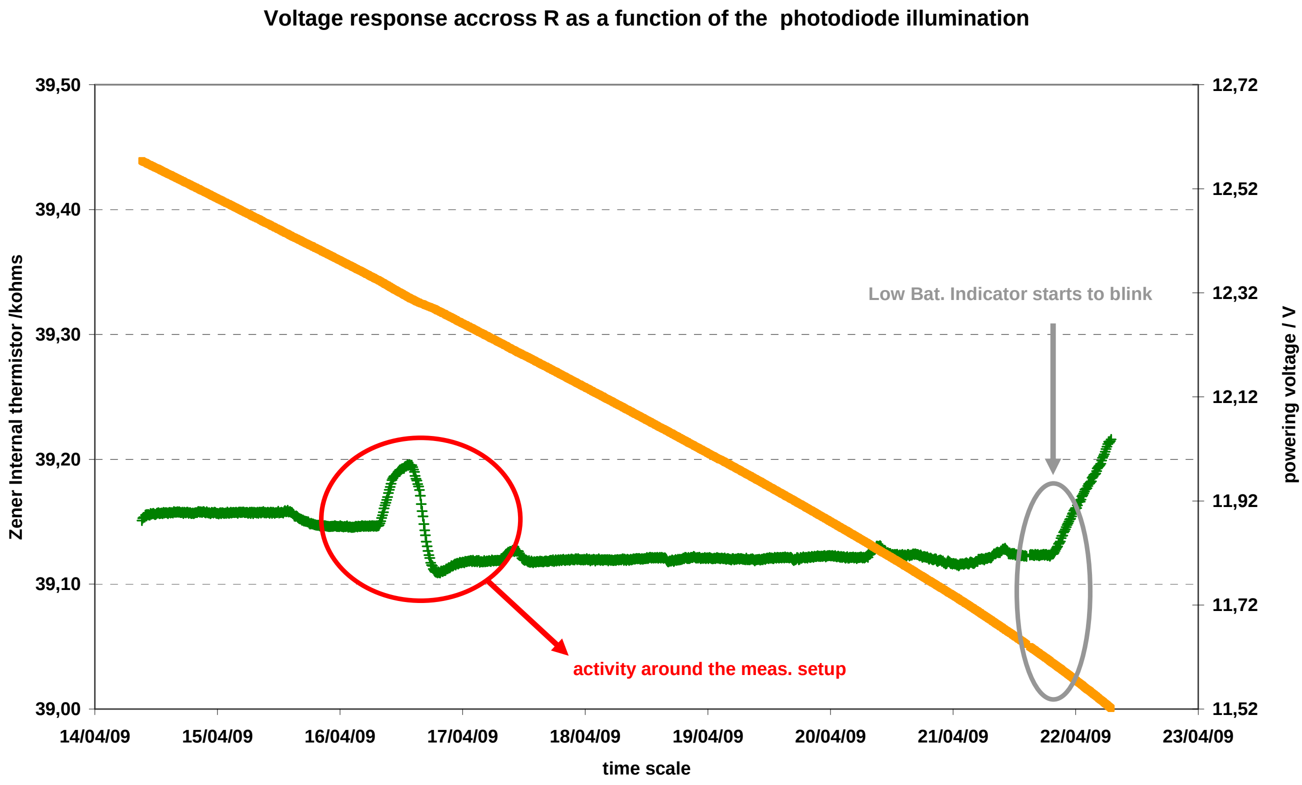

Graph B3 Evolution of the voltage across the powering batteries (orange), and the internal temperature of the Zener (green) as a function of time.